

Grain growth behavior at absolute zero during nanocrystalline metal indentation

F. Sansoz^{a)} and V. Dupont*School of Engineering, The University of Vermont, Burlington, Vermont 05405*

(Received 5 June 2006; accepted 21 July 2006; published online 12 September 2006)

The authors show using atomistic simulations that stress-driven grain growth can be obtained in the athermal limit during nanocrystalline aluminum indentation. They find that the grain growth results from rotation of nanograins and propagation of shear bands. Together, these mechanisms are shown to lead to the unstable migration of grain boundaries via process of coupled motion. An analytical model is used to explain this behavior based on the atomic-level shear stress acting on the interfaces during the shear band propagation. This study sheds light on the atomic mechanism at play during the abnormal grain coarsening observed at low temperature in nanocrystalline metals. © 2006 American Institute of Physics. [DOI: 10.1063/1.2352725]

Intense grain refinement can promote drastic changes of plasticity mechanism in bulk materials and thin films.^{1–8} In metals containing nanosized grains (<100 nm), several independent experiments have recently revealed abnormal grain coarsening phenomena at room temperature under large applied stress.^{9–16} Surprisingly, during microindentation, this coarsening effect was found to occur faster at cryogenic temperatures.¹¹ This finding is opposite to the thermodynamics of grain growth commonly observed in coarse-grained materials.¹⁷ The underlying mechanism(s) governing the abnormal coarsening of nanograins during indentation, however, remained an open question.

In order to investigate the atomic mechanism of indentation-induced grain growth at very low temperature, we perform a numerical experiment: With the aid of concurrent multiscale simulations, we investigate the indentation process with the total exclusion of thermally assisted mechanism. We perform molecular static simulations of indentation at absolute zero (0 K) using the quasicontinuum method;¹⁸ details on this numerical procedure are provided elsewhere.¹⁹ In this letter, we simulate the indentation of 200-nm-thick films subjected to a perfectly rigid 15 nm radius cylindrical indenter using an embedded-atom-method potential for Al.²⁰ Thin films with either single crystal or columnar grain structures are investigated. In the latter case, all simulated grain boundaries are tilt boundaries and the grains have a random in-plane crystal orientation. The nanocrystalline models investigated have average grain sizes of 5 and 7 nm.

The indentation response at zero temperature is found to differ markedly between single crystal and nanocrystalline Al (Fig. 1). In the single crystal film, the onset of plasticity is characterized by a single dislocation pop-in event,²¹ while the plasticity of the nanocrystalline metals is governed by flow serrations. Our simulations confirm that the serrated yielding observed in the nanocrystalline metals is directly caused by the formation of thin shear bands under the contact interface, which is largely in agreement with the models proposed in the literature.^{7,22} The shear bands are formed by sliding of several aligned grain boundaries and concurrently extend by intragranular slip into the grains that are in the prolongation of the band. The intragranular slip is found to

be dominated by the emission and propagation of partial dislocations, each leaving an extended stacking fault along its path.³ The formed stacking faults are also found to initiate the growth of deformation twins.⁴ The propagation of the shear bands is clearly indicative that a significant shear flow is operative over distances much larger than the average grain size under consideration.

We also explore the atomic mechanisms of deformation at larger depths of indentation. It is manifested from the study of the two grain sizes investigated that motion of grain boundaries and disappearance of nanosized grains occur simultaneously during shear band propagation. For brevity, in the following, we only focus our analysis of the deformation processes on a representative cluster of grains in the 7 nm grain size model [dashed area in Fig. 2(a)]. Figures 2(b)–2(h) show the evolution of the structure of this grain cluster during indentation. In these figures, the force value in the lower-

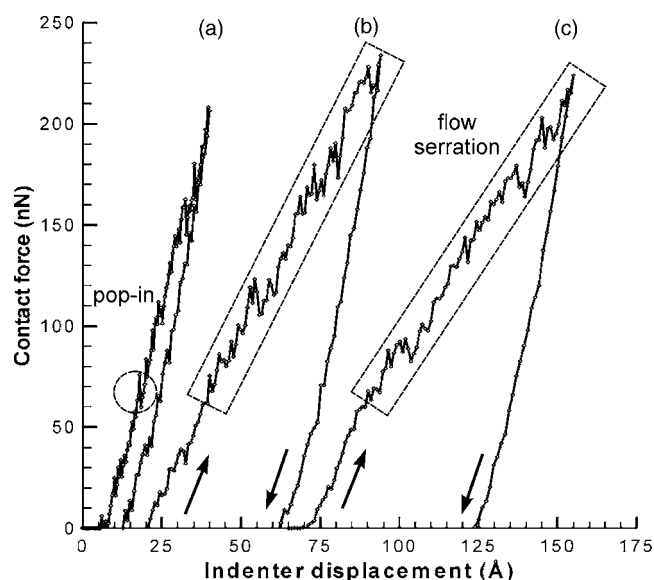


FIG. 1. Loading and unloading indentation responses of Al films at absolute zero simulated by quasicontinuum method. (a) Single crystal film. Film plasticity occurring by typical dislocation pop-in events. Dashed circle corresponds to the emission of the first dislocation. (b) 5 nm grain size film. (c) 7 nm grain size film. Nanocrystalline metal response characterized by flow serration is indicative of the propagation of shear bands. Curves (b) and (c) have been shifted to the right for clarity.

^{a)}Electronic mail: frederic.sansoz@uvm.edu

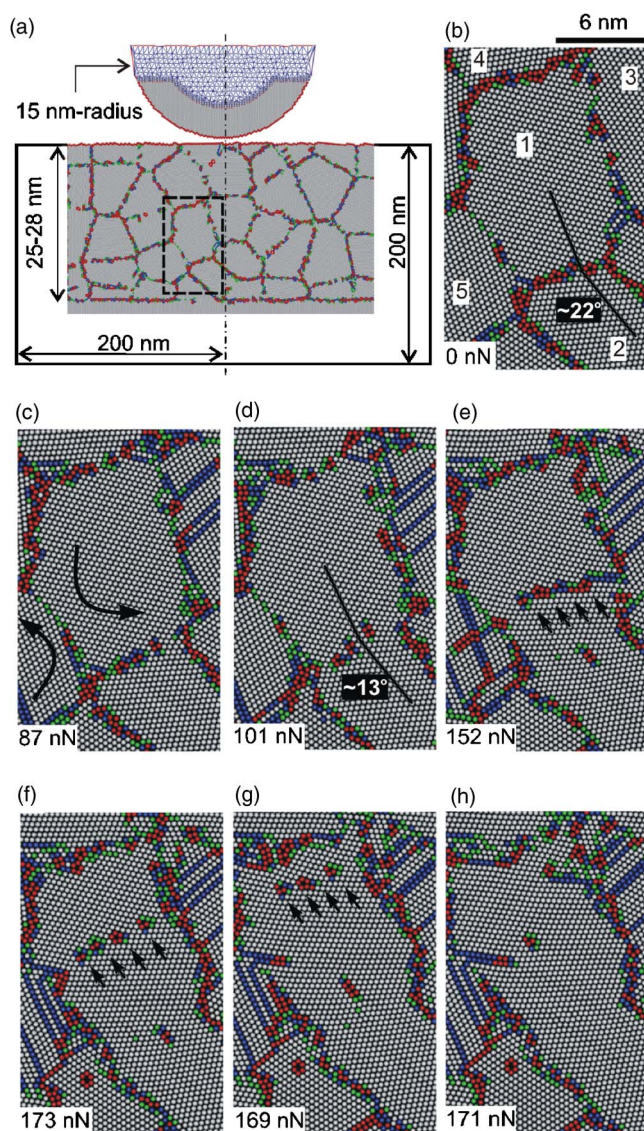


FIG. 2. (Color online) Deformation of a representative grain cluster in the prolongation of a shear band in the 7 nm grain size Al film. (a) Contact zone before indentation. Dimensions and location of the fully refined atomistic region are indicated with respect to the atomistically informed finite element domain (not to scale). Dashed area showing the location of the grain cluster. [(b)–(d)] Rotation of grain 1. [(e)–(h)] Motion of the boundary separating grains 1 and 2. The applied contact force is indicated in the lower-left corner of the images. The color scheme used for each atom corresponds to the centrosymmetry parameter (Ref. 21).

left corner of the images represents the contact force applied by the indenter to the film. Early in the indentation process, significant rotation of grain 1 (central grain) takes place due to grain boundary sliding between grains 1 and 5 (left grain), as shown in Fig. 2(c). It is also important to note that the structure of the grain boundaries changes significantly during grain rotation. More specifically, grains 1 and 2 (lower grain) are separated by a high-angle grain boundary (misorientation angle between grains of $\sim 22^\circ$) before initial indentation [Fig. 2(b)]; but the same boundary is transformed into a low-angle grain boundary (misorientation angle of $\sim 13.5^\circ$) after grain 1 rotation. In addition, grain 1 is in the prolongation of a shear band, which is noticeable by the presence of stacking faults in grain 3 (right grain) that are represented by blue atom lines inside this grain [Fig. 2(c)]. As the contact force exerted by the indenter increases, there is clear evidence of

motion of the boundary separating grains 1 and 2. This boundary begins to migrate in the direction normal to its plane until it is absorbed by the interface made with grain 4 (upper grain). The atomic mechanism of migration is accomplished by local lattice rotations forming vortexlike patterns similar to those found in fluid shear flows [Fig. 3(a)]. Therefore, the lattice atoms of grain 1 are collectively shuffled across the interface to become atoms arranged in the lattice of grain 2. In this process, grain 2 grows while grain 1 tends to disappear. The grain boundary motion necessitates several loading increments in order to be completed. Furthermore, upon unloading, only one grain remains. A possible interpretation of this result is that the grain boundary motion becomes rapidly unstable as shown below.

One can calculate the shear stress causing migration of a tilt boundary as a function of tilt misorientation between grains using the theory developed by Gutkin and Ovid'ko.²³ This theory predicts the minimum external shear stress causing stable interface motion and an estimate of the larger shear stress leading to unstable grain boundary motion. The latter is given by

$$\tau_{c2} \approx \frac{0.8G\omega}{2\pi(1-\nu)}, \quad (1)$$

where G denotes the shear modulus, ν Poisson's ratio, and ω the tilt misorientation between grains. For the migration problem described above, using $G=32$ GPa, $\nu=0.31$, and $\omega=13.5^\circ$, we find that the critical shear stress τ_{c2} is equal to 696 MPa. This value is compared to the orientation of the boundary plane between grains 1 and 2 [Fig. 3(b)]. Each stress map represented in Fig. 3(b) corresponds to a different loading level taken from the rotation of grain 1 (top left) to the complete disappearance of this grain (bottom right). From this figure, it is evident that the local shear stress gradient causing the migration of the interface between the two grains becomes significantly larger than the unstable critical shear stress τ_{c2} calculated above. This result is also supported by the fact that the contact force becomes almost constant or even decreases when the interface is displaced beyond the center of the grain [Figs. 2(f)–2(h)]. Consequently, it is found that the interface migration process causes a strong stress relief in the grain boundary network similar to that found in the superplasticity studies of microscale Al alloys.²⁴ Furthermore, a direct effect of the stress relief is the tangential translation of grain 1 relative to grain 2, which is indicated by horizontal arrows on the left boundary of grain 1 in Fig. 3(b). This effect clearly suggests that the mechanism of stress-assisted grain growth found in the present study corresponds to the normal motion of grain boundaries resulting from a shear stress applied tangential to them and causing tangential motion, a mechanism referred to as coupled motion of grain boundaries.^{25–27}

Earlier theoretical works have been conducted using molecular dynamics simulation to understand the mechanisms of indentation in fully three-dimensional nanocrystalline metal films at zero and finite temperatures.^{28,29} No atomistic studies, however, have shown the occurrence of grain growth under indentation at very low temperature. Here, we have used a multiscale simulation method which helps investigating large depths of indentation in thin films. As a result, it has been possible to simulate the propagation of shear bands which are found to play a key role on the coupled motion of

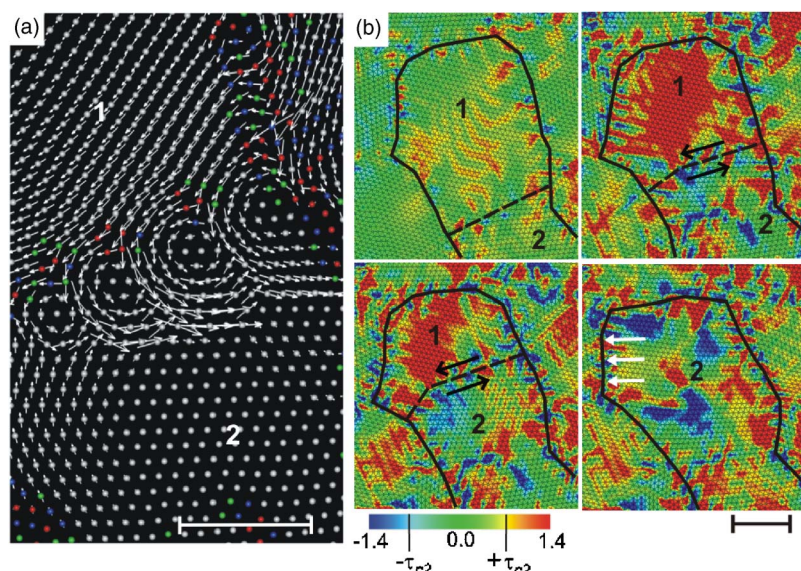


FIG. 3. (Color online) (a) Magnitude and orientation of the atomic trajectories between two loading increments during the motion of the boundary separating grains 1 and 2. Coupled boundary motion via local lattice rotations forming vortexlike patterns. (b) Atomic-level shear stress with respect to the orientation of the interface between grains 1 and 2 at different stages of the boundary motion (in units of GPa). The boundaries of grains 1 and 2 have been highlighted for clarity. τ_{c2} is the critical stress value leading to unstable boundary motion. Grain boundary motion produces stress relief in the grain cluster. Note in the bottom-right image that the tangential motion of grain 1 (represented by light-colored arrows) parallel to its moving interface also indicates that the grain boundary motion is coupled. Scale bars are 3 nm.

the grain boundaries. This mechanism is certainly different from that of curvature-driven grain growth and rotation-induced grain coalescence, which have been suggested in the past for the grain growth observed in nanocrystalline metals.^{12,30} More specifically, the latter mechanism would have required more significant grain rotation in order to be accomplished.³⁰ Coupled motion of grain boundaries has been investigated both theoretically²⁵ and by atomistic simulation^{26,27} in infinitely long bicrystals made of pure metal. Here, it is shown that coupled grain boundary motion is also an important mode of deformation in nanocrystalline materials under stress, which can account for grain coarsening phenomena in the absence of thermally activated processes. Understanding the fundamental mechanism leading to stress-assisted grain growth in nanocrystalline materials will show considerable promise toward achieving superplasticity in thin film materials.

This work was conducted under the auspices of the Vermont Experimental Program to Stimulate Competitive Research (VT EPSCoR) under Grant No. NSF EPS 0236976. The authors would like to thank Yves Dubief for helpful comments during the preparation of the manuscript.

¹J. Schiotz, F. D. Di Tolla, and K. W. Jacobsen, *Nature (London)* **391**, 561 (1998).

²L. Lu, M. L. Sui, and K. Lu, *Science* **287**, 1463 (2000).

³V. Yamakov, D. Wolf, S. R. Phillpot, A. K. Mukherjee, and H. Gleiter, *Nat. Mater.* **1**, 45 (2002).

⁴M. W. Chen, E. Ma, K. J. Hemker, Y. M. Wang, and X. Cheng, *Science* **300**, 1275 (2003).

⁵J. Schiotz and K. W. Jacobsen, *Science* **301**, 1357 (2003).

⁶K. S. Kumar, S. Suresh, M. F. Chisholm, J. A. Horton, and P. Wang, *Acta Mater.* **51**, 387 (2003).

⁷A. Hasnaoui, H. Van Swygenhoven, and P. M. Derlet, *Science* **300**, 1550 (2003).

⁸X. Huang, N. Hansen, and N. Tsuji, *Science* **312**, 249 (2006).

⁹M. Jin, A. M. Minor, E. A. Stach, and J. W. Morris, Jr., *Acta Mater.* **52**, 5381 (2004).

¹⁰K. Zhang, J. R. Weertman, and J. A. Eastman, *Appl. Phys. Lett.* **85**, 5197 (2004).

¹¹K. Zhang, J. R. Weertman, and J. A. Eastman, *Appl. Phys. Lett.* **87**, 061921 (2005).

¹²Q. Wei, D. Jia, K. T. Ramesh, and E. Ma, *Appl. Phys. Lett.* **81**, 1240 (2002).

¹³Z. Shan, E. A. Stach, J. M. K. Wiezorek, J. A. Knapp, D. M. Follstaedt, and S. X. Mao, *Science* **305**, 654 (2004).

¹⁴X. Z. Liao, A. R. Kilmametov, R. Z. Valiev, H. S. Gao, X. D. Li, A. K. Mukherjee, J. F. Bingert, and Y. T. Zhu, *Appl. Phys. Lett.* **88**, 021909 (2006).

¹⁵D. S. Gianola, S. Van Petegem, M. Legros, S. Brandstetter, H. Van Swygenhoven, and K. J. Hemker, *Acta Mater.* **54**, 2253 (2006).

¹⁶G. J. Fan, Y. D. Wang, L. F. Fu, H. Choo, P. K. Liaw, Y. Ren, and N. D. Browning, *Appl. Phys. Lett.* **88**, 171914 (2006).

¹⁷G. Gottstein and L. S. Shvindlerman, *Grain boundary Migration in Metals: Thermodynamics, Kinetics, Applications* (CRC, Boca Raton, FL, 1998).

¹⁸R. Miller and E. B. Tadmor, *J. Comput.-Aided Mater. Des.* **9**, 203 (2002).

¹⁹V. Dupont and F. Sansoz, *Mater. Res. Soc. Symp. Proc.* **903E**, 0903-Z06-05.1 (2005).

²⁰A. F. Voter and S. P. Chen, *Mater. Res. Soc. Symp. Proc.* **82**, 175 (1987).

²¹C. L. Kelchner, S. J. Plimpton, and J. C. Hamilton, *Phys. Rev. B* **58**, 11085 (1998).

²²A. C. Lund and C. A. Schuh, *Mater. Res. Soc. Symp. Proc.* **806**, MM7.4.1 (2004).

²³M. Y. Gutkin and I. A. Ovid'ko, *Appl. Phys. Lett.* **87**, 251916 (2005).

²⁴L. M. Dougherty, I. M. Robertson, and J. S. Vetrano, *Acta Mater.* **51**, 4367 (2003).

²⁵J. W. Cahn and J. E. Taylor, *Acta Mater.* **52**, 4887 (2004).

²⁶A. Suzuki and Y. Mishin, *Mater. Sci. Forum* **502**, 157 (2005).

²⁷F. Sansoz and J. F. Molinari, *Acta Mater.* **53**, 1931 (2005).

²⁸D. Feichtinger, P. M. Derlet, and H. Van Swygenhoven, *Phys. Rev. B* **67**, 024113 (2003).

²⁹X. L. Ma and W. Yang, *Nanotechnology* **14**, 1208 (2003).

³⁰A. J. Haslam, D. Moldovan, V. Yamakov, D. Wolf, S. R. Phillpot, and H. Gleiter, *Acta Mater.* **51**, 2097 (2003).